Atmospheric Research 109-110 (2012) 36–51

Contents lists available at SciVerse ScienceDirect

Atmospheric Research

journal homepage: www.elsevier.com/locate/atmos

Effects of SST magnitude and gradient on typhoon tracks around East Asia: A case study for Typhoon Maemi (2003)

Kyung-Sook Yun[a], Johnny C.L. Chan[b], Kyung-Ja Ha[a,*]

[a] Division of Earth Environmental System, College of Natural Science, Pusan National University, Busan, Korea
[b] Guy Carpenter Asia-Pacific Climate Impact Centre, School of Energy and Environment, City University of Hong Kong, Hong Kong, China

ARTICLE INFO

Article history:
Received 14 June 2011
Received in revised form 8 February 2012
Accepted 9 February 2012

Keywords:
TC track
SST magnitude
SST gradient
East Asia
Potential vorticity tendency

ABSTRACT

The effects of sea surface temperature (SST) magnitude and horizontal gradient of SST on the northeastward typhoon motion around East Asia are investigated in a case for Typhoon Maemi (2003), using the Weather Research and Forecasting (WRF) model. The effects of SST on tropical cyclone (TC) motion are explained using the concept of potential vorticity tendency (PVT), which provides a good dynamical explanation for the TC motion. A warm SST significantly strengthens the TC intensity and induces a greater eastward drift in the TC motion. Asymmetry in the PVT reveals the maximum to the northeast and the minimum to the southwest, implying the northeastward-moving TC motion. A warmer SST induces a greater eastward deflection of the maximum PVT. The change in the PVT is primarily due to the horizontal advection of the cyclonic vortex rather than diabatic heating or vertical advection. Southwesterly flow advects the TC northeastward more effectively as SST magnitude is increased. In addition, a zonal SST increase from west to east produces a larger eastward deflection in the TC motion than a meridional SST gradient and a SST magnitude. Compared to the other SST gradients, the SST increase from west to east is more favorable for the southwestward tilt of the vortex axis and the resultant vertical southeasterly wind shear. Consequently, this SST gradient may induce a greater eastward drift in the TC motion owing to the enhancement of asymmetric vortex and flow.

1. Introduction

Tropical cyclones (TCs) have destructive effects on the industry and infrastructure of large cities and local communities. Increasing global mean temperatures have led to increased social and economic interest in the possible changes in the intensity and track of TCs (Marks and Shay, 1998). In particular, sea surface temperature (SST) could induce a significant increase in the intensity of TCs through an enhanced thermodynamic energy supply (e.g., Emanuel, 1986; Holland, 1997; Pereira Filho et al., 2010). However, relationship between TC motion and SST variations has not yet been sufficiently explored.

Earlier studies (Chang and Madala, 1980; Tuleya and Kurihara, 1982) have shown SST to be an important factor affecting TC motion. A high SST contributes to the genesis and intensification of TCs (Emanuel, 1986; Chan et al., 2001). Tuleya and Kurihara (1982) reported that a warm SST increases the TC intensity and induces a northwestward shift of the northwestward-moving TC related to the beta effect (sensitive to the intensity and size of the TC). However, it is difficult to explain the change in TC motion on the basis of the beta effect alone. Wu et al. (2005) showed the relative contribution of the symmetric and asymmetric SST components to TC motion. They demonstrated that the asymmetric SST component modulates the TC motion by changing the asymmetry in rainfall and vertical motion, while the symmetric component is related to the beta effect. This result indicates the importance of the asymmetric distributions of SST on TC motion. Chang and Madala (1980) presented evidence that the spatial distribution of SST influences the TC motion, a

* Corresponding author at: Department of Atmospheric Sciences, Pusan National University, Busan 609-735, Korea. Tel.: +82 51 510 2177; fax: +82 51 515 1689.
E-mail address: kjha@pusan.ac.kr (K.-J. Ha).

0169-8095/$ – see front matter © 2012 Elsevier B.V. All rights reserved.
doi:10.1016/j.atmosres.2012.02.012

warm SST to the right of the mean flow is more favorable for the northwest drift of westward-moving TCs than a warm SST on the left side.

TC motion is principally modulated by two dynamical mechanisms: advection of potential vorticity by large-scale environmental flows and beta drift associated with the planetary vorticity gradient (e.g., Chan and Williams, 1987; Fiorino and Elsberry, 1989; Chan et al., 2002). Large-scale environmental flow basically moves a TC downstream, whereas the beta drift in the northern hemisphere tends to cause a northwestward motion in all directions of TC propagation. If the direction of the environmental flow is opposite to that of the beta effect, the balance between the two would be important for determining the direction of TC motion. In addition, convective heating can significantly affect TC motion through the direct asymmetric heating and the asymmetric flow caused by diabatic heating (Flatau et al., 1994; Wu et al., 2005). Recently, it has been found that terrain can also affect the TC track and landfall (Kuo et al., 2001; Wong and Chan, 2006; Au-Yeung and Chan, 2010). TCs tend to drift toward land, and this has been explained by strong asymmetries in the friction, heat, and moisture between land and sea.

Under certain environmental mean flows and topographic effects, SST may exert a distinct effect on TC motion. Although the several earlier studies have investigated the SST impact on TC motion (e.g., Chang and Madala, 1980; Tuleya and Kurihara, 1982), the dynamical processes of the SST impact on the TC track are not investigated further. In the present study, we investigate the dynamical processes for the TC motion in terms of the spatial distribution of SST. To explain the dynamics, changes in different terms of potential vorticity tendency (PVT) and vertical structure of the vortex are investigated. The PVT framework explains the internal and external dynamics, which includes the environmental steering flow, the beta-induced circulation, and the advection of asymmetric PV by the symmetric flow (Chan et al., 2002). In addition, this study aims to investigate the SST effect on track with a particular focus to the TC embedded in environmental flow around East Asia. Although most previous studies are based on a simple idealized environmental condition owing to the advantage in the interpretation of the dynamical process, the environmental factors for real TC can provide different perspectives of SST effect on TC intensity and track through the interaction with the environmental factors (e.g., Wang and Wu, 2004). For accurate prediction of TC motion, dynamical processes on TC motion should be investigated under different SST distributions. To isolate the SST effect in a realistic environmental situation, we use the Weather Research and Forecasting (WRF) model; initial and boundary conditions are prescribed specifically for the case of Typhoon Maemi which passed over the Korean Peninsula in 2003. The numerical experiment results indicate the impact of SST magnitude and horizontal gradient of SST on the TC motion around East Asia.

2. Model and method

2.1. Model description and experiment

To examine the effects of SST on the TC motion around East Asia, TC motion is simulated using WRF 3.2 with different SSTs but the same initial values and boundary conditions. The horizontal grid resolution is 15 km with 180×173 grids in the horizontal and 28 full-sigma (σ) levels in the vertical. For the physical processes, the WRF single-moment 6-class scheme (WSM6) and the Yonsei University planetary boundary layer (PBL) scheme (i.e., non-local-K scheme with an explicit entrainment layer and parabolic K profile in the unstable mixed layer) (Hong et al., 2006) are used. Surface layer physics follow Monin–Obukhov with a Carlson–Boland viscous sub-layer and standard similarity functions. The Kain–Fritsch scheme (Kain and Fritsch, 1990), which has both deep and shallow sub-grid convection using a mass flux approach with downdrafts and convective available potential energy (CAPE) removal time scale, is employed for cumulus parameterization. The model top is set to 50 hPa. Initial and boundary conditions are provided by the National Centers for Environmental Prediction Final (NCEP FNL) operational global analysis data (6 hourly, $1.0^\circ \times 1.0^\circ$).

We focus on the TC motion around East Asia. For realistic simulation of the TCs affecting East Asia, the basic state of the atmosphere and the initial/boundary atmospheric conditions of the experiments are given by those for Typhoon Maemi (2003), which generated record-breaking heavy rainfall and strong winds over East Asia from 00 UTC 11 to 00 UTC 13 September 2003. The model is integrated over 72 h with a time step of 60 s, from 00 UTC 10 to 00 UTC 13 September 2003. The SST in the control (CTL) experiment is set to the initial SST condition provided by the FNL data for Typhoon Maemi; the SST mean averaged over all model domains is approximately 300 K (Fig. 2a). The CTL simulation replicates well the observed best-track from the Joint Typhoon Warning Center (JTWC) (Fig. 1). In order to isolate the effects of SST magnitude, experiments are run for SSTs ranging from 290 K to 310 K at 2.5 K intervals. For example, the SST in EXP_T302.5 is uniform at 302.5 K over all model domains, as shown in Fig. 2b. To understand the impact of the horizontal SST gradients, experiments with a positive and negative SST gradient in the north-south and east-west directions are also carried out. The SST gradient is set at about 0.3 K/100 km, and the SST distributions are shown in Fig. 2c–f. The experimental designs are listed in Table 1. Basically, EXP_GSN exhibits the most realistic SST gradient, while EXP_GNS, EXP_GEW, EXP_GWE are somewhat unrealistic. The horizontal gradient of SST in reality during September is usually from about 0.3 K/100 km to 0.5 K/100 km, corresponding to the SST gradient prescribed in the experiments. Although the SST gradients are somewhat unrealistic, this was designed to simplify the dynamical interpretation for the TC track associated with the anomalous SST change in the zonal and meridional directions.

2.2. Potential vorticity tendency

Wu and Wang (2000) have demonstrated that the TC motion follows the local maximum in the azimuthal wavenumber-1(WN1) potential vorticity tendency (PVT). The PVT provides a good dynamical explanation for the TC motion mechanism (Chan et al., 2002). The potential vorticity

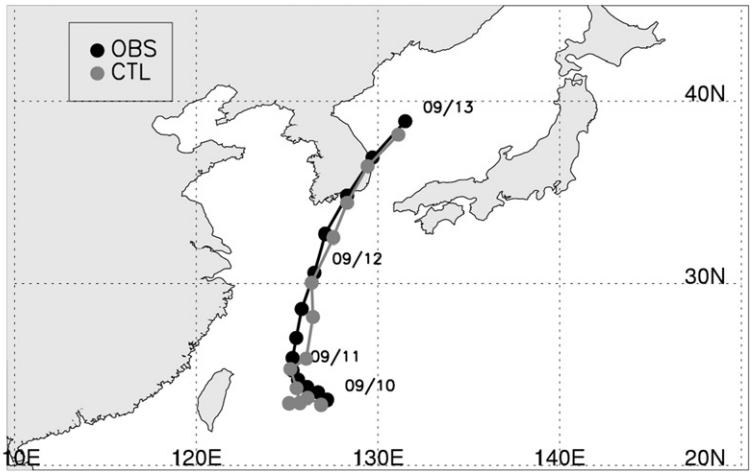

Fig. 1. Comparison of best tracks (OBS) with simulated tracks in CTL for Typhoon Maemi (2003).

(P) and its tendency ($\frac{\partial P}{\partial t}$) are defined in sigma coordinates, as follows:

$$P = -\frac{g}{p_s}\left[(\zeta + f)\frac{\partial \theta}{\partial \sigma} + \frac{\partial u}{\partial \sigma}\frac{\partial \theta}{\partial y} - \frac{\partial v}{\partial \sigma}\frac{\partial \theta}{\partial x}\right] \quad (1)$$

$$\frac{\partial P}{\partial t} = -u\frac{\partial P}{\partial x} - v\frac{\partial P}{\partial y} - \dot{\sigma}\frac{\partial P}{\partial \sigma} + \frac{g}{p_s}\left[-(\zeta + f)\frac{\partial \dot{\theta}}{\partial \sigma} - \frac{\partial u}{\partial \sigma}\frac{\partial \dot{\theta}}{\partial y} + \frac{\partial v}{\partial \sigma}\frac{\partial \dot{\theta}}{\partial x}\right] \quad (2)$$

where $\dot{\sigma}$is the vertical velocity in sigma coordinates, $\dot{\theta}$ is the rate of change of the potential temperature, and the remaining symbols have their usual meanings. The terms on the right-hand side of Eq. (2) are horizontal advection (HA) (first two terms), vertical advection (VA), and diabatic heating (DH), respectively. Since the effect of friction can be neglected above the boundary layer, the three terms contribute to the PVT. The details are given in Wu and Wang (2000).

For the sake of brevity, the layers are divided into a boundary layer (BL; $1.0 \geq \sigma \geq 0.9$), a lower layer (LL; $0.9 \geq \sigma \geq 0.55$), and an upper layer (UL; $0.55 \geq \sigma \geq 0.25$), as in Wong and Chan (2006). The PVT was first calculated in Cartesian coordinate, and it was transferred into that in cylindrical coordinate. All the terms are then Fourier-decomposed to obtain the WN1 component (i.e., the asymmetric component with respect to the TC center). Finally, the PVT was again transferred into that in Cartesian coordinate. To determine the TC track, the TC center could be defined as the center position of the minimum pressure or the maximum potential vorticity (PV). Basically, the position of the minimum pressure is consistent with that of the maximum PV. However, Wong and Chan (2004) demonstrate that the minimum pressure is more appropriate for defining the TC center than the maximum PV does, because the PV is relatively large near the strong updraft and has a weak asymmetry with respect to the origin of the surface TC center. As a result, the TC center is identified as the center position of the minimum pressure at the surface. Because our main interest is the average TC motion, the results are mainly displayed by daily composites from the hourly model data. As shown in Fig. 1, the TC track is translated from northwestward to northeastward after the 24 h. To focus the northeastward moving motion after the translation, the results on the second day (i.e., hours 24–48) are displayed. In addition, the model simulation has the equilibrium time in the spin-up process of about 24 h. Note that on the third day, the TC makes landfall and it can induce different friction and moisture dynamics on TC motion. For this reason, we have chosen the second day to do the daily composites.

3. Sensitivity to SST magnitude

As noted in previous studies (e.g., Tuleya and Kurihara, 1982; Emanuel, 1986), the TC intensity is sensitive to the SST magnitude because of the changes in lower-level temperature and moisture. Fig. 3b displays the temporal evolution of minimum sea level pressure (SLP) in the CTL and EXP runs. In fact, the CTL experiment fails to simulate the observed TC intensity (figure not shown), because of the lack of a deep understanding of the physical processes/mechanisms to TC intensity. Regardless of the different intensity, the similar track between observation and simulation (see Fig. 1) may be due to a large steering effect of the environmental flow. The results suggest that a warmer SST induces a stronger TC intensity. The intensity in EXP_T302.5 (SST of ~29.4 °C) is similar to that in the CTL run. This could be a result of the similar SST value over the domain (see Fig. 2a and b). The response to the SST magnitude is larger in the experiments with SST above 302.5 K (EXP_T305, EXP_T307.5, and EXP_T310). The differences in intensity between the CTL and EXP runs at SSTs above 300 K (~26.9 °C) increase nearly monotonically until about 48 h (the equilibrium time). In short, an SST increase of 2.5 K produces an intensity increase of about 25–35 hPa at 48 h (~10–14 hPa K^{-1}). This corresponds reasonably well with the rate of intensification in previous studies (e.g., Holland, 1997; Chan et al., 2001). As reported by Chan et al. (2001), the rate of intensification decreases at SSTs above 305 K (31.9 °C). This decrease in the rate of intensification may be related to a thermodynamic limitation on the SST warming-induced TC intensification. Chan et al. (2001) also obtained a similar thermodynamical

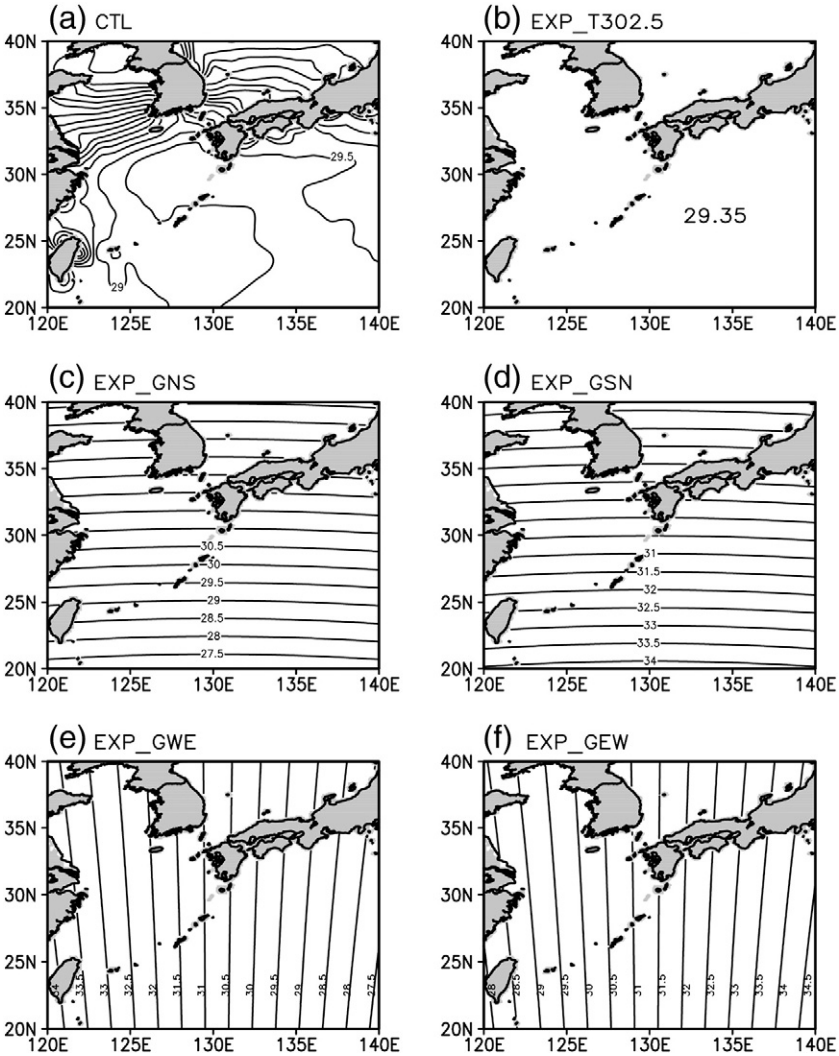

Fig. 2. SST distribution (unit: °C) in (a) CTL, (b) EXP_T302.5, (c) EXP_GNS, (d) EXP_GSN, (e) EXP_GWE, and (f) EXP_GEW. The experiment designs are listed in Table 1.

limitation on TC intensification, using a simple ocean–atmosphere coupled model with different model physics. This suggests that the threshold is not simply determined by the specification of physics incorporated into the WRF. To understand this in detail, more investigation on the possible limitation may be necessary in the future study. For an SST below 300 K, however, there are slight changes: the intensity in EXP_T297.5 (~24.4 °C) is roughly similar to that in the experiments with lower SST values (EXP_T295, EXP_T292.5, and EXP_T290), and the intensity decrease is restricted to within ~40 hPa. This noteworthy change in the intensity may be related to the critical value of SST for TC formation and development, which has been suggested as the threshold of approximately 26.8 °C (Wendland, 1977).

Table 1
Experimental design for WRF 3.2 model.

EXP		SST condition
CTL		Initial condition of SST provided by FNL data
SST magnitude	EXP_T290	Uniform at 290 K
	EXP_T292.5	Uniform at 292.5 K
	…	Change with 2.5 K range
	EXP_T307.5	Uniform at 307.5 K
	EXP_T310	Uniform at 310 K
SST gradient	EXP_GNS	Increased SST from south to north
	EXP_GSN	Decreased SST from south to north
	EXP_GWE	Increased SST from east to west
	EXP_GEW	Decreased SST from east to west

In regard to the enhanced TC intensity, the TC track appears to significantly change. To show the impact of SST magnitude on the TC track, the track is represented by the smallest (EXP_T290) and largest (EXP_T310) SST values with the CTL run (Fig. 3a). The TC track exhibits larger differences in the east–west distance than in the north–south distance. Although the change in the track is more complex than that in intensity, the difference in the zonal distance between the CTL and EXP runs is consistent with the intensity change shown in Fig. 3b (Fig. 3c). An SST that is warmer (cooler) than 302.5 K leads to a larger eastward (westward)

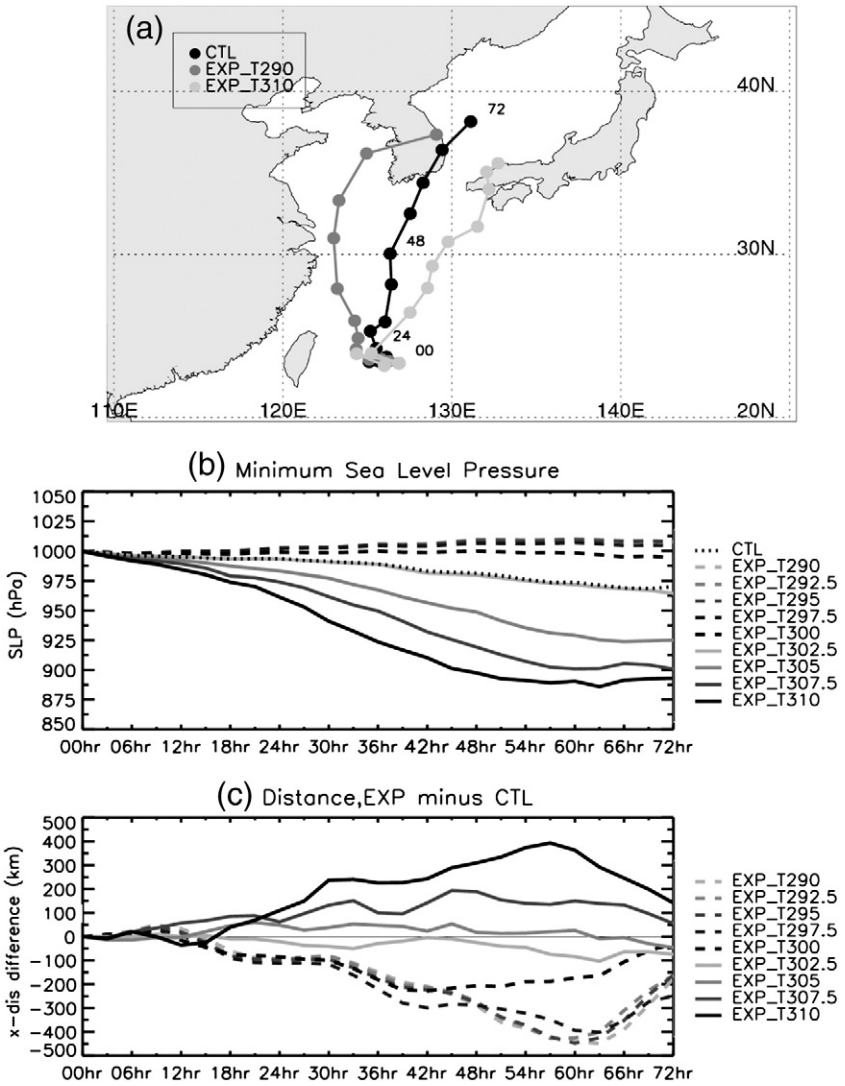

Fig. 3. (a) Simulated track from CTL (black line), EXP_T290 (dark gray line), and EXP_310 (light gray line). (b) Temporal variations of minimum sea level pressure (unit: hPa) at TC center in CTL and EXP experiments. (c) Same as (b), but for EXP minus CTL difference of zonal distance for TC center (unit: km).

drift relative to the CTL run. For example, at 60 h, an SST warmer by ~7.5 K results in an eastward deflection of ~400 km (i.e., the difference between EXP_T310 and EXP_T302.5). Tuleya and Kurihara (1982) have shown that a warmer SST induces a greater northward shift of westward-moving TCs. Their result coincides with the east deflection of northward-moving TCs, in the sense of rightward drift of the TC-propagating direction. The experiment results averaged during 24–48 h are summarized in Table 2.

While the change in the TC intensity is easily explained by the enhanced thermodynamic energy supply, the change in the TC track may be modulated by a more complex dynamical process. Previous studies (Adem, 1956; Chan and Williams, 1987; Fiorino and Elsberry, 1989) have demonstrated that the beta effect, which is sensitive to the intensity and size (strength and area of outer wind) of the vortex, causes TC to drift to the north and west relative to the mean wind in all propagating directions of the northern hemisphere. Tuleya and Kurihara (1982) concluded that a warmer SST leads to a stronger vortex intensity and beta effect and eventually causes the northwestward movement of the northwestward-moving TC. While the beta effect causes the northwestward movement of the TC in all propagating directions of the northern hemisphere, in this study, the TC

Table 2
Summary of experiment results averaged during 24–48 h on SST magnitude.

	Intensity from CTL (hPa)	X-distance from CTL (km)	U-wind shear (m/s)	V-wind shear (m/s)
CTL	0	0	−9.6	5.9
EXP_T297.5	16.2	−207.9	3.4	−1.1
EXP_T300	11.5	−163.3	0.2	2.1
EXP_T302.5	−0.9	−26.2	−8.8	4.5
EXP_T305	−21.1	39.0	−10.6	5.7
EXP_T307.5	−40.1	129.0	−11.8	4.6

basically moves northeastward, and a warmer SST produces a greater eastward drift. The eastward deflection of the TC motion should therefore be the result of other dynamical causes. To investigate the dynamical causes for the TC motion, we adopt the WN1 PVT approach (e.g., Wu and Wang, 2000; Chan et al., 2002). It was previously reported that the WN1 components of PVT with respect to the TC center represent the asymmetries generated by advection and diabatic heating and thereby shift the TC to the area of maximum PVT. Fig. 4 shows the WN1 PVT at the LL in CTL and experiments with SSTs in the range from 297.5 K to 307.5 K averaged during the second day (hours 24–48). Basically, the asymmetries in PVT have a different magnitude order in relation to the TC intensity. To find the change of the maximum position in PVT, the contour intervals are differently shown in Fig. 4. The WN1 PVT in CTL exhibits a positive value to the northeast and a negative value to the southwest. The asymmetry in the PVT suggests that the TC tends to move toward the northeast, which is consistent with the TC track shown in Fig. 2a. The tendency in CTL (Fig. 4a) resembles the southwest–northeast asymmetry in EXP_T302.5 (Fig. 4d). Although the direction of the maximum PVT does not exactly correspond to the TC motion, there is a systematic eastward drift of the maximum PVT as SST is increased. In comparison with the PVT in the EXP_T302.5, a warmer SST causes the eastward drift of the maximum PVT. A cooler SST than 302.5 K induces a relatively weak westward drift of the maximum PVT compared to that in the CTL run. Some

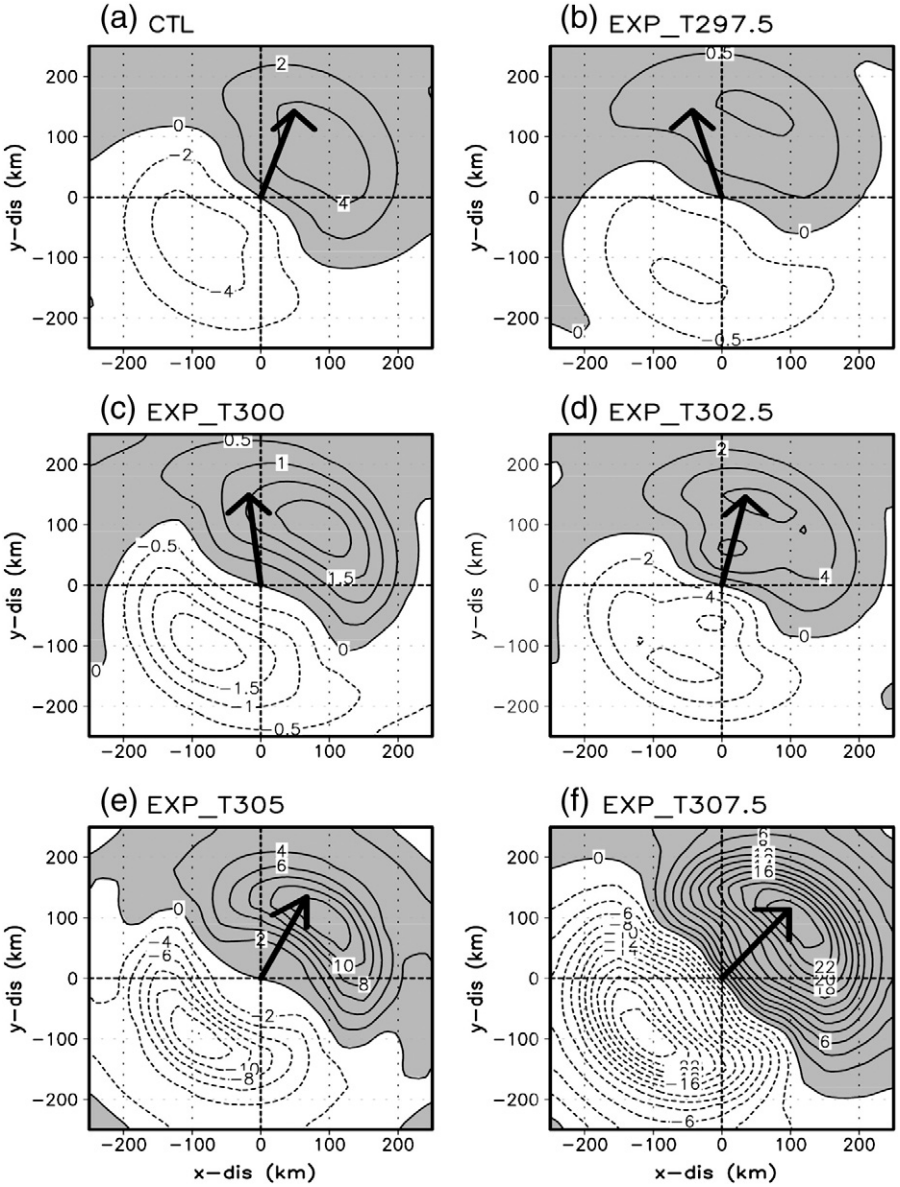

Fig. 4. Wavenumber-1 component of time composite of LL average of potential vorticity tendency for (a) CTL and (b–f) EXP experiments on SST magnitude on the second day. Positive values are shaded. The contour interval is (a, d, e, and f) 2.0, (b and c) 0.5, respectively (unit: 10^5 PVU s^{-1}).

inconsistencies between the TC motion direction and WN1 PVT maximum may be contributed by rapid changes in the TC motion direction throughout the simulation.

As mentioned in Section 2.2, the PVT has three main contributions: horizontal advection (HA), vertical advection (VA), and diabatic heating (DH). To illustrate the individual contributions of these phenomena to the PVT, we show the horizontal distribution of the HA, VA, and DH terms in EXP_T297.5, CTL, and EXP_T307.5 in Fig. 5. The HA term in CTL exhibits a maximum to the northeast and a minimum to the southwest, while the DH term is roughly opposite to the HA term but with a smaller magnitude. The VA term has an irregular asymmetry and a smaller magnitude compared to the HA and DH terms. Consequently, the HA term dominates the PVT change and tends to move the TC northeastward. In EXP_T307.5 (EXP_T297.5) with a warmer (cooler) SST, the HA term is remarkably shifted to the east (west) with a stronger (weaker) asymmetry. This drift in the HA term well explains the total PVT change and thus the direction of the TC motion.

Note that previous studies (e.g., Willoughby, 1990; Wu and Wang, 2000; Wu et al., 2005) have emphasized the role of the DH term in modulating the direction of the TC motion. Since diabatic heating is deeply associated with total rainfall, we display in Fig. 6 the temporal variation of the hourly rainfall averaged within 100 km of the surface TC center along all directions (E, S, W, and N). An evident anticlockwise turning of the position of maximum rainfall occurs in the CTL run (Fig. 6a). For example, the core of maximum rainfall gradually moves from the northeast to the southwest of the TC center during hours 30–42. However, because the rotation of the rainfall pattern shows a weaker tendency from the southwest to the northeast, the area of maximum rainfall is slightly situated to the southwest. For this reason, as SST magnitude is increased (Fig. 6b to d), rainfall asymmetry is shifted southwestward, corresponding to the direction of the maximum DH term.

Chan et al. (2002) have reported that when the steering by environmental flow is strong, the DH term has an insignificant impact on the TC motion, and therefore, the TC motion is mostly dominated by the HA term. To identify the effect

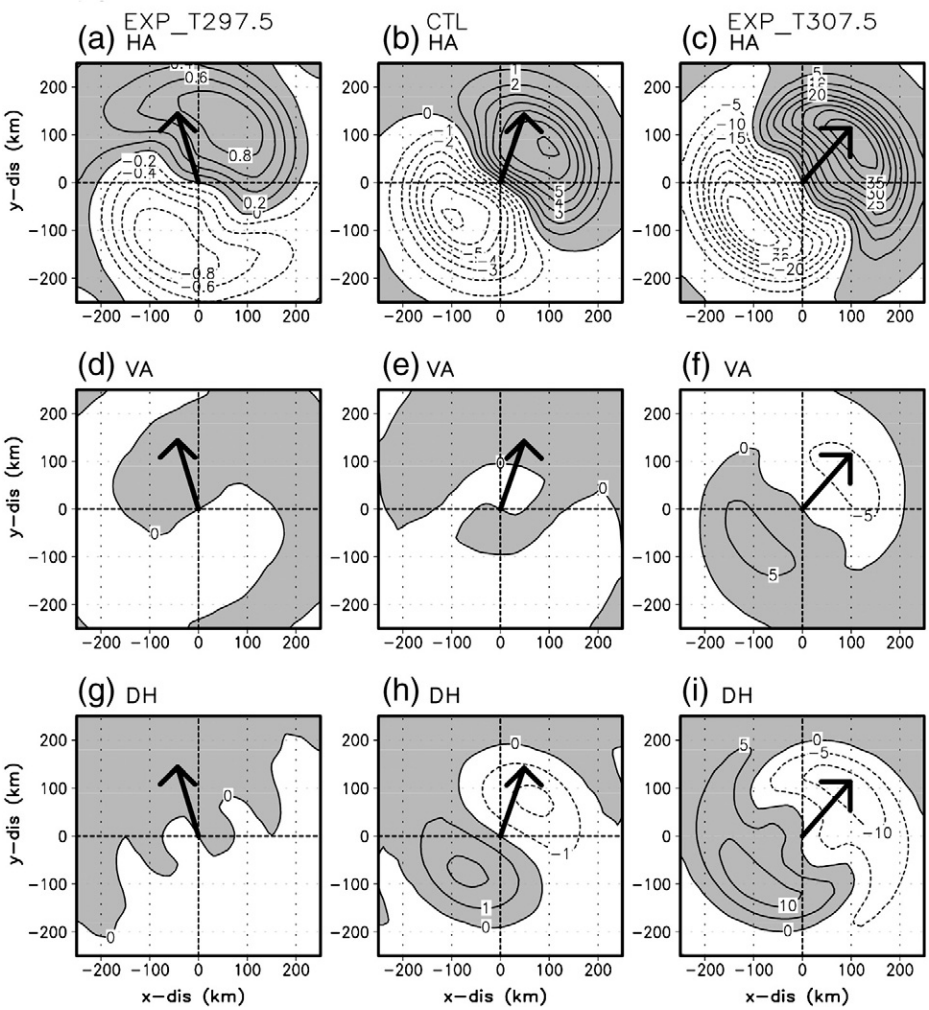

Fig. 5. Wavenumber-1 component of time composite of LL average of the terms in potential vorticity tendency for (a, d, and g) EXP_T295.7, (b, e, and h) CTL, and (c, f, and i) EXP_T307.5 experiments on SST magnitude on the second day: (a–c) horizontal advection term, (d–f) vertical advection term, and (g–i) diabatic heating term. Positive values are shaded. The contour interval is (a, d, and g) 0.2, (b, e, and h) 1.0, and (c, f, and i) 5.0, respectively (unit: 10^5 PVU s^{-1}).

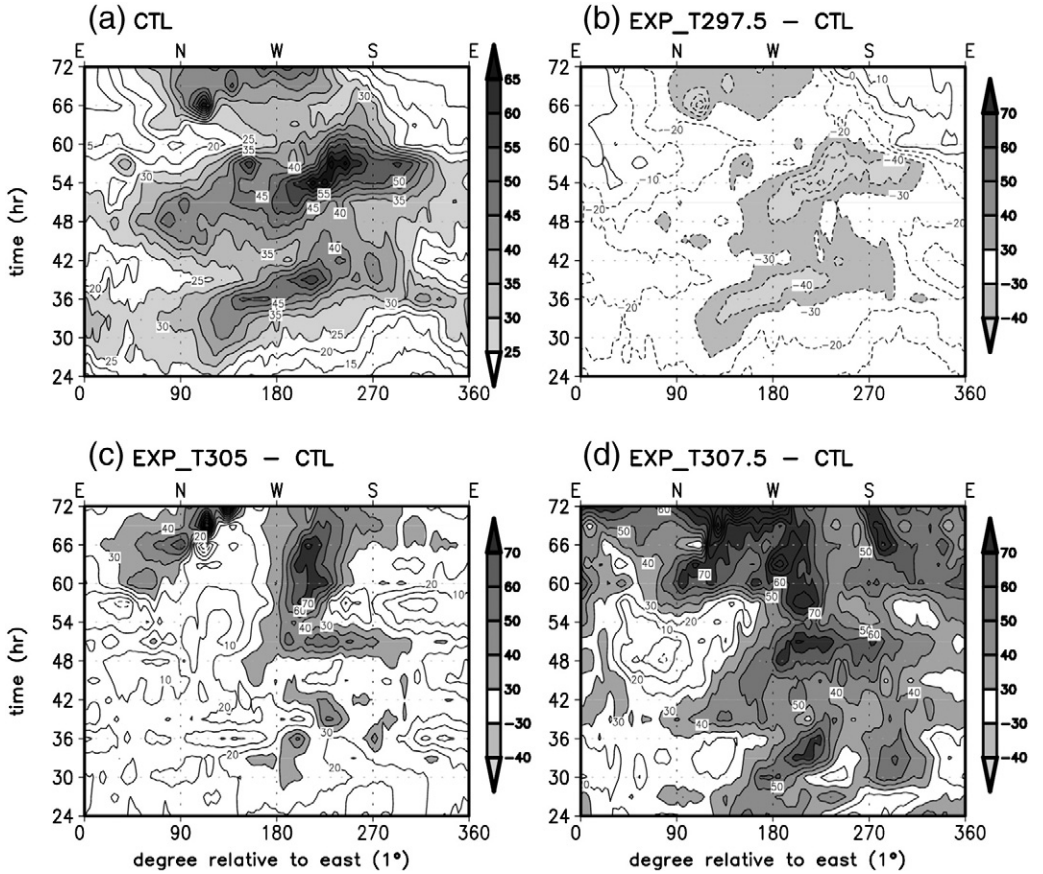

Fig. 6. (a) Time–azimuth variations of rainfall averaged within 100 km of TC surface center at each azimuth for CTL experiment. (b–d) Same as (a), but for difference between CTL and (b) EXP_T297.5, (c) EXP_T305, and (d) EXP_T307.5. Abscissa on top of each panel indicates degree relative to east with four cardinal directions (E, S, W, and N).

of the environmental flow on the HA term, total wind and its asymmetric flow at the LL in EXP_T297.5, CTL, and EXP_T307.5 are shown in Fig. 7. Here, the asymmetric flow is calculated by subtracting the symmetric wind, with respect to the TC center, from the total wind field. In CTL (Fig. 7c), the maximum of wind speed leans horizontally to the southeast with respect to the TC center. The resultant southwesterly flow is prominent in the asymmetric wind (Fig. 7d). The TC is primarily steered by the southwesterly flow. In the experiment with a cooler SST (EXP_T297.5), the maximum of the strong wind is located to the east. As the result, the asymmetric westerly flow is reduced in comparison to that in CTL. On the other hand, in the experiment with a warmer SST (EXP_T307.5), the asymmetric southwesterly flow is significantly enhanced. The southwesterly steering flow, which is enhanced at a high SST magnitude, could advect the cyclonic vortex northeastward more effectively. The result supports the claim that the HA term is the primary contributor to the PVT and the resulting northeastward TC motion.

In addition to the PVT change, it was reported in earlier studies (e.g., Wang and Holland, 1996; Wong and Chan, 2004) that the vertical structure in the vortex is closely connected with the TC motion, through changes in the vertical shear and the secondary circulation. To show the vertical structure in the vortex, we calculate the PV and its asymmetric component in the zonal-height (meridional-height) section averaged within meridionally (zonally) 100 km from the surface TC center (Fig. 8). While the PV asymmetry is relatively symmetric at the lower level, evident asymmetries appear in the upper level. As a result, at the upper level in CTL, the maximum PV is located to the west and south, while the minimum is located to the east and north (Fig. 8c and d). Because the asymmetries at the upper-level are directly related to the vertical tilt of the vortex (e.g., Frank and Ritchie, 2001), this occurs with a significant southwestward tilt of the vortex axis. A warmer SST (Fig. 8e and f) strengthens the southwestward tilt, while a cooler SST (Fig. 8a and b) induces the northeastward tilt of the vortex axis.

The tilt of the vortex axis and the resultant asymmetry can produce a significant change in the vertical wind shear. From the earlier studies (Jones, 1995; Bender, 1997), it was known that the asymmetry in the vortex is significantly related to the vertical wind shear. Fig. 9 presents the vertical profile of the zonal and meridional winds averaged within 100 km of the surface TC center. There exist easterly and southerly wind shear (i.e., increased easterly and southerly with increasing height) in CTL. To compare the results quantitatively, the vertical wind shears between 200 hPa and 850 hPa are represented in Table 2. The SST greater than 302.5 K exhibits a significant easterly and southerly shear.

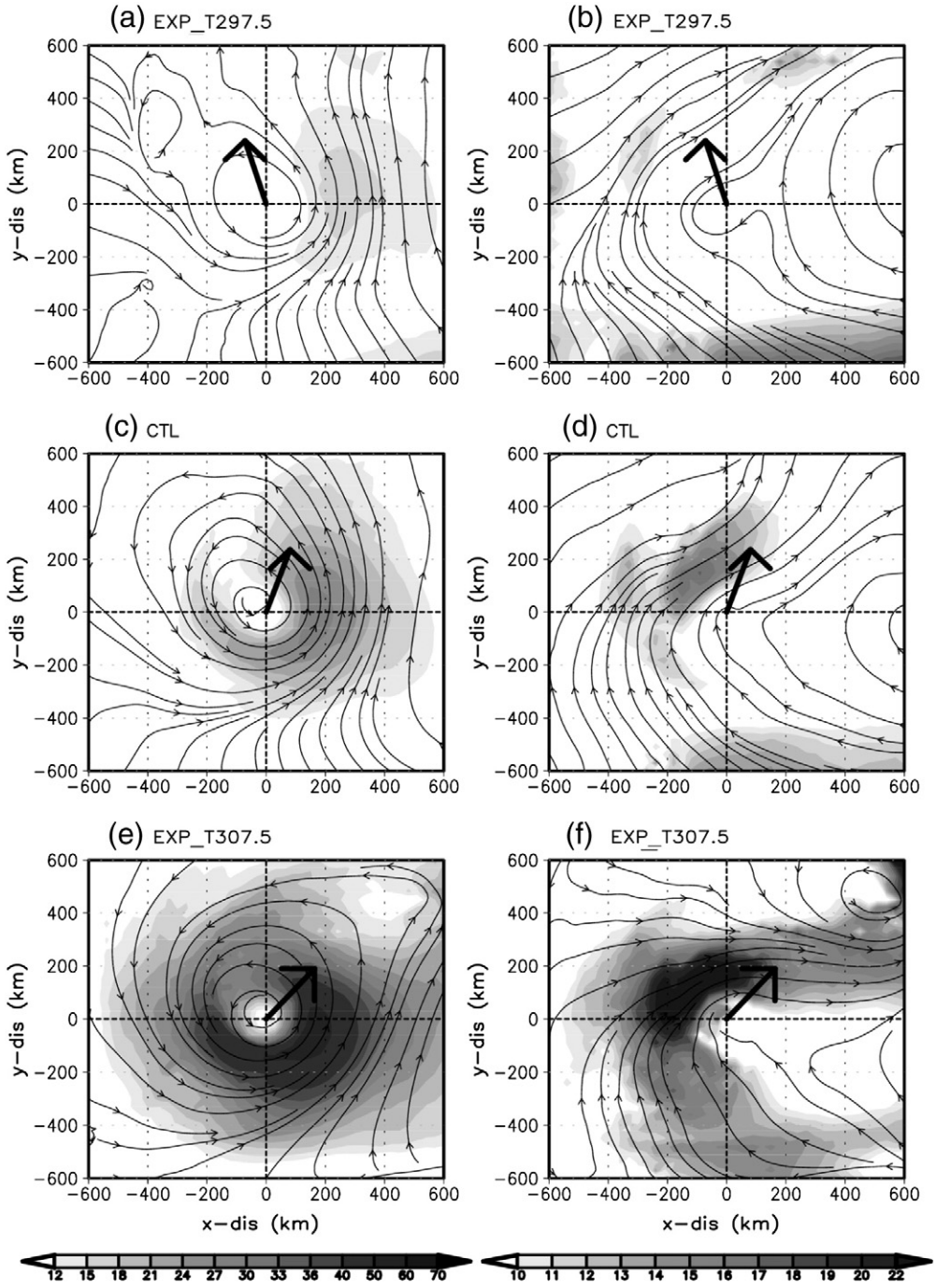

Fig. 7. Composite of (a, c, and e) total wind flow and (b, d, and f) asymmetric flow (stream line) at LL for (a–b) EXP_T297.5, (c–d) CTL, and (e–f) EXP_T307.5 on the second day. Shading indicates speed of the flow (unit: ms^{-1}).

Notice that the vertically shear structure has strong effects on the asymmetry in convection and rainfall. It was reported that asymmetry in convection and rainfall is oriented to the left (clockwise) of the vertical wind shear (e.g., Frank and Ritchie, 2001). The maximum to the southwest in DH term (see Fig. 5) agrees well with the direction of vertical shear. A warmer SST roughly forms a stronger easterly and southerly wind shear. Meanwhile, a more intense TC is related to higher vertical shear. Although the vertical shear can inhibit TC intensification, the TCs may still intensify in substantial vertical shear if the SST is high (e.g., Black et al., 2002).

4. Impact of horizontal gradient of SST

We now investigate the impact of the zonal and meridional SST gradients on the TC motion. To identify which

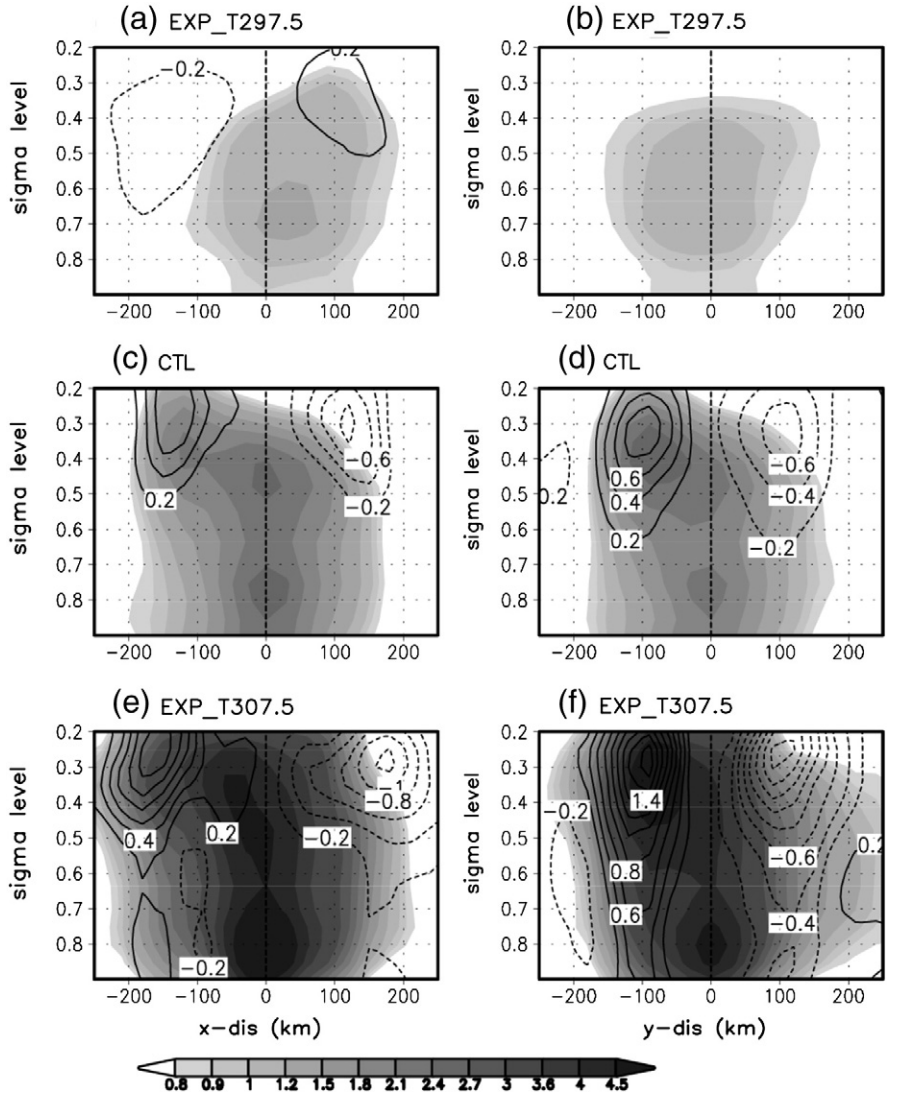

Fig. 8. (a, c, and e) Zonal-height and (b, d, and f) meridional-height cross section of potential vorticity (shading; unit: PVU) and its asymmetric component(contour) averaged within (a, c, and e) meridional and (b, d, and f) zonal direction of 100 km from surface TC center for (a–b) EXP_T297.5, (c–d) CTL, and (e-f) EXP_T307.5 on the second day.

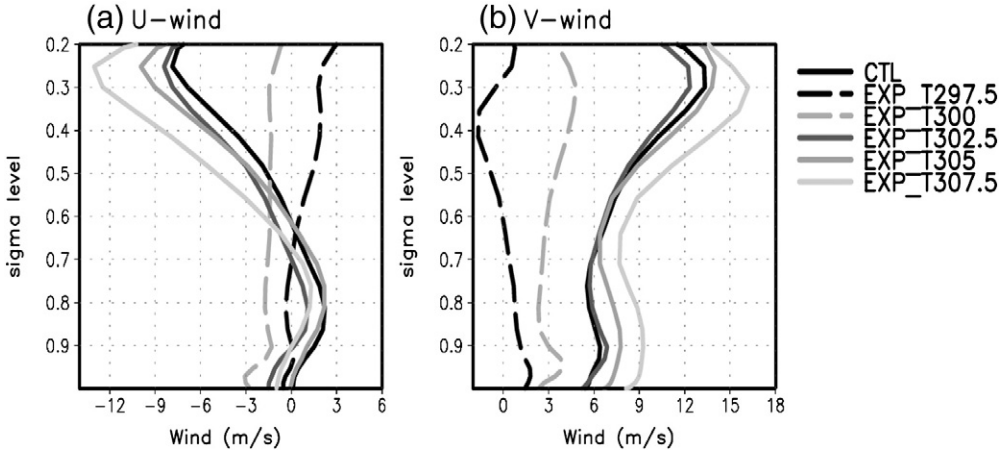

Fig. 9. Vertical structure of (a) zonal and (b) meridional winds averaged within 100 km of surface TC center for experiments on SST magnitude on the second day.

component of the magnitude and gradient is more important in modulating the TC motion, we design experiments with different initial SST values. In other words, the SST in EXP_GNS increases from the south to the north and the SST magnitude at the location [25°N, 125°E] (~302.5 K) is cooler than that in EXP_GSN (~305 K). In addition, the SST in EXP_GEW increases from the west to the east and the SST magnitude at the location [25°N, 125°E] (~302.5 K) is cooler than that in EXP_GWE (~305 K).

As in the result for the SST magnitude, the change in intensity roughly follows the SST magnitude, regardless of the gradient: EXP_GWE and EXP_GSN with a warmer SST exhibit a stronger intensity than do EXP_GEW and EXP_GNS (Fig. 10b). The change in the intensity is also similar to that shown in Fig. 3b. However, the change in the track poses significant differences between the zonal and meridional gradients. Despite the cooler SST, the zonally increased SST relative to the TC-moving direction (i.e., EXP_GEW) tends to cause the TC to drift eastward (Fig. 10a). The eastward movement (~500 km) caused by the SST increase from west to east in Fig. 10c is greater than the eastward deflection (~400 km) caused by the SST warming of 7.5 K in Fig. 3c. The other experiments do not show any significant track change compared to EXP_GEW. Note that the meridional SST gradients roughly generate the track change in relation to the TC intensity (i.e., an intense TC induces an eastward movement of TC). Despite the warmer SST magnitude, the decreased zonal gradient in EXP_GWE tends to move the TC slightly westward. This result suggests that the SST increase from west to east is important in determining the direction of TC

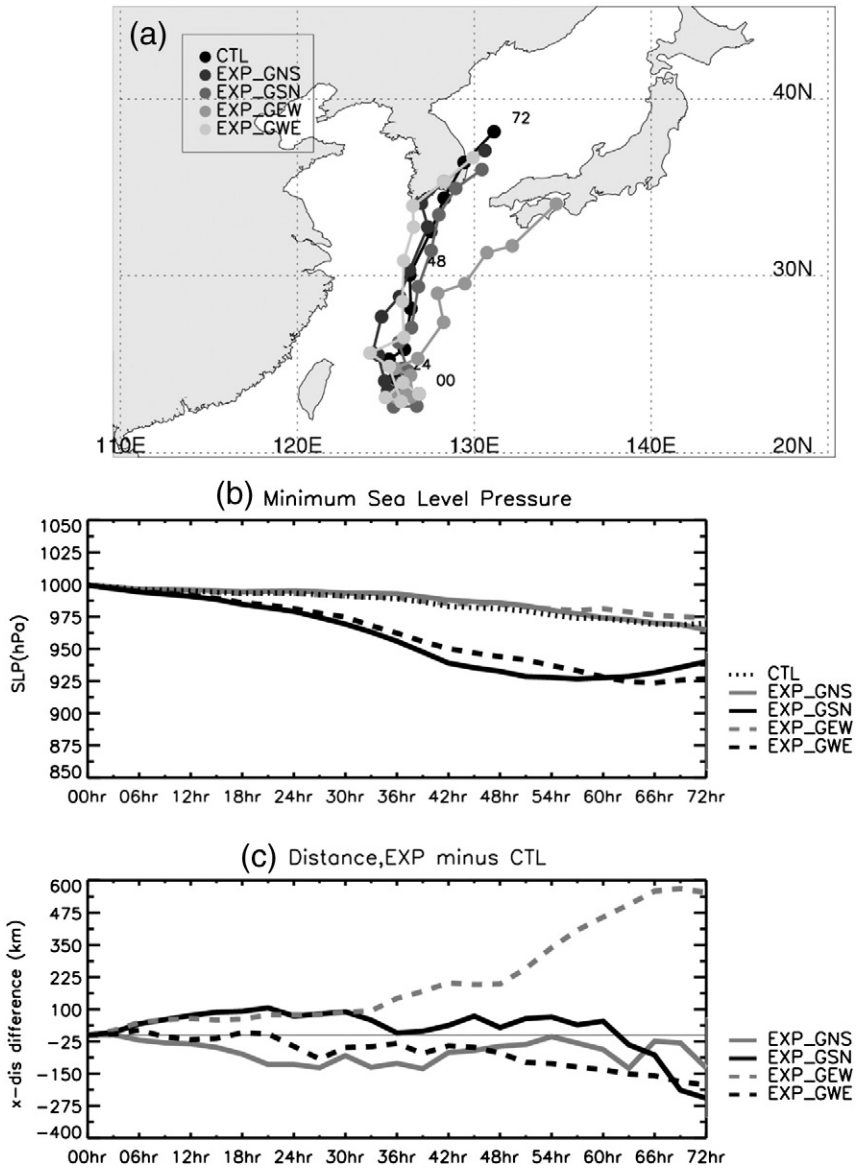

Fig. 10. (a) Simulated track from CTL, EXP_GNS, EXP_GSN, EXP_GWE, and EXP_GEW. (b) Temporal variations of EXP minus CTL difference for minimum sea level pressure (unit: hPa) on TC center. (c) Same as (b), but for zonal distance from CTL TC center (unit: km).

Table 3
Summary of experiment results averaged during 24–48 h on SST gradient. Here, the wind shears between 200 hPa and 850 hPa are averaged during 24–48 (48–72) h.

	Intensity from CTL (hPa)	X-distance from CTL (km)	U-wind shear (m/s)	V-wind shear (m/s)
EXP_GNS	3.5	−73.4	−10.3 (−5.8)	4.2 (6.7)
EXP_GSN	−32.5	51.9	−1.9 (2.1)	2.4 (−2.4)
EXP_GWE	−25.3	−55.0	−5.6 (3.8)	−0.8 (−4.8)
EXP_GEW	1.1	138.9	−10.7 (−9.4)	4.8 (13.0)

motion around East Asia. The experiment results averaged during 24–48 h on the SST gradients are summarized in Table 3. In an earlier study, Chang and Madala (1980) concluded that a warmer SST on the right of the mean flow induces a stronger intensity of westward-moving TCs and causes the TCs to drift into warmer-SST regions than does a SST on the left of the mean flow. The results reported by Chang and Madala (1980) are remarkably consistent with our main finding, namely, the translating TC is sensitive to the SST gradient perpendicular to the mean flow.

Fig. 11 presents the WN1 PVT at the LL in EXP_GNS, EXP_GSN, EXP_GWE, and EXP_GEW, averaged during the second day. The increase in the zonal SST from west to east (Fig. 11d) has a greater eastward deflection of the maximum PVT in comparison to that in CTL (Fig. 4a). It is consistent with the definite eastward translation of the TC. On the other hand, the experiments with the other SST gradients (Fig. 11a–c) do not reveal the greater eastward deflection of the maximum PVT. For example, the asymmetric PVT structure in Fig. 11a shows a larger northwestward deflection, implying a larger northwestward movement of the TC. The asymmetries of PVT in Fig. 11b and c are similar to that in CTL, although the magnitudes are significantly larger. The greater eastward deflection of the positive PVT in EXP_GEW is mostly attributed to the HA term (figure not shown).

How does the zonal SST gradient drive the larger eastward drift of the TC motion? Indeed, the movement of TCs results in asymmetries of the TC structure. To answer this question, we investigate the zonal and meridional asymmetries in the vortex (Fig. 12). As shown in Fig. 8, the vortex has originally a cyclonic asymmetry (positive PV) to the southwest and an anticyclonic asymmetry (negative PV) to the northeast. In fact, the asymmetric vortex generates the asymmetry in the temperature (figure not shown): the temperature is warmer to the northeast and cooler to the southwest with respect to the TC center. The increased SSTs relative to the TC moving direction in the zonal and meridional directions (i.e., EXP_GEW and EXP_GNS) agree closely with the asymmetric temperature in the vortex. Consequently, these increased SSTs favor the southwestward tilt of the vortex axis. In other words, the vortices in EXP_GNS

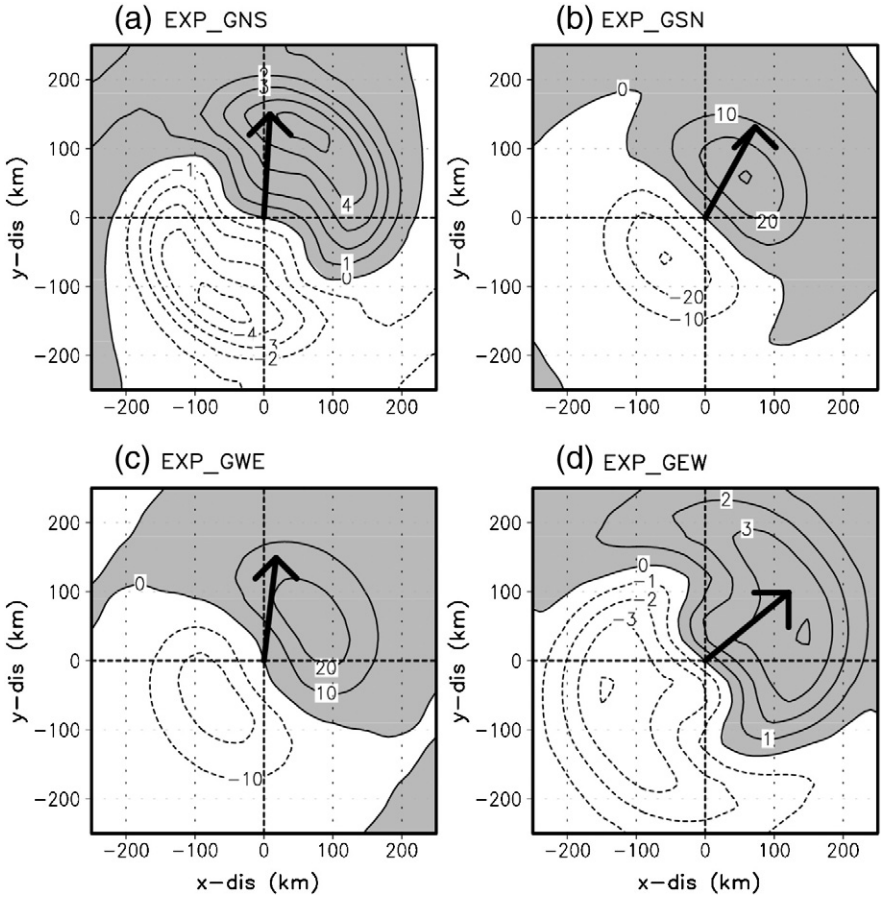

Fig. 11. Same as Fig. 4, but for experiments on SST gradient. The contour interval is (a and d) 1.0, (b and c) 10.0, respectively.

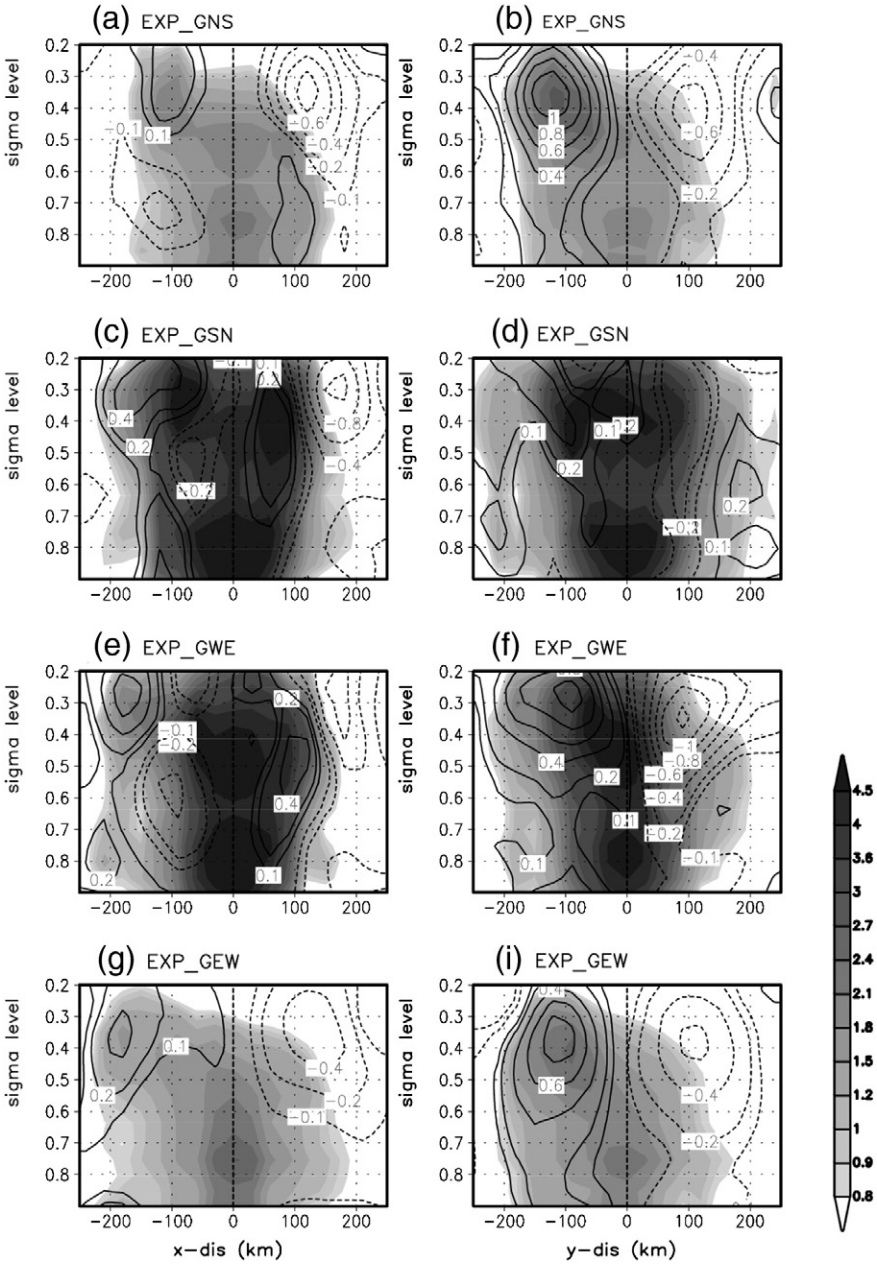

Fig. 12. Same as Fig. 8, but for experiments on SST gradient.

and EXP_GEW tilt to the southwest (Fig. 12a–b and g–h), while those in EXP_GSN and EXP_GWE do not show any westward tilt (Fig. 12c–d and e–f). In particular, the vortex in EXP_GEW (Fig. 12g) has a coherent westward tilt vertically, while that in EXP_GNS (Fig. 12a) shows an eastward tilt in the lower-level. The vortex tilt to the southwest appears to be most significant in the increased zonal SST from west to east (EXP_GEW). The eastward drift of the TC motion could be related to the development of the asymmetric vortex and flow, caused by the vertical tilt of the vortex axis.

The direction of the vertical wind shear is remarkably consistent with the vertical tilt of the vortex (Fig. 13). The strong upper-level asymmetry is related to the strong vertical wind shear. The decreased SSTs in the translating direction(EXP_GWE and EXP_GSN) do not show a coherent easterly and southerly shear through 24 to 72 h (Fig. 13). On the other hand, although the TC intensity is relatively weak, the increased SSTs in the translating direction (EXP_GEW and EXP_GNS) induce a significant easterly and southerly wind shear throughout the simulation, as represented in Table 3. The significant easterly and southerly shear is more evident in EXP_GEW than in EXP_GNS, corresponding to the greater eastward movement in EXP_GEW. Although the effect of the vertical wind shear on the TC track is somewhat complex, the vortex asymmetry with

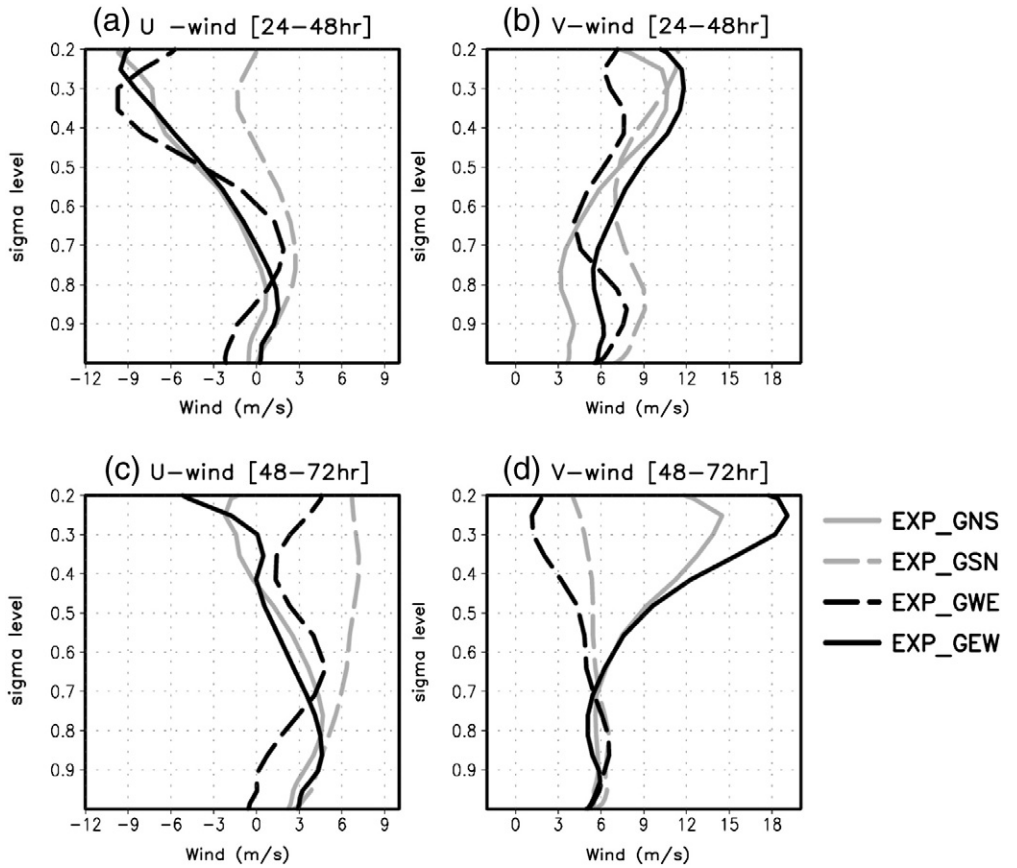

Fig. 13. Vertical structure of (a, c) zonal and (b, d) meridional winds averaged within 100 km of surface TC center for experiments on SST magnitude on the (a–b) second day and (c–d) third day.

the vertical wind shear has significant effects on the motion of TCs (Wang and Holland, 1996; Ritchie and Frank, 2007; Zheng et al., 2007). For example, Ritchie and Frank (2007) have shown that a persistent north–northwesterly shear develops over the TC center as a result of an interaction between the primary circulations of TC and gradient of absolute vorticity, which is related to the motion of TCs to the northwest. Consequently, this southeasterly shear can induce a strong asymmetric flow and in turn contribute to the greater eastward movement of TC. Note that the meridionally increased SST in EXP_GNS does not cause an apparent eastward movement, despite the easterly and southerly wind shear. It may be concluded that the TC motion to the east of the moving direction is more important for air–sea energy exchanges (e.g., asymmetric evaporation and convective heating) than that to the north, south, or west (Chang and Madala, 1980).

5. Discussion and conclusion

On the basis of numerical experiments, we investigate the effects of the SST magnitude and horizontal gradient of SST on the northeastward TC motion with a particular focus to the TC embedded in environmental flow around East Asia. For this, initial and boundary conditions are prescribed specifically for the real case of Typhoon Maemi in 2003. The TC track change is controlled by internal dynamics (e.g., convective asymmetry, vertical structure/circulation, vortex Rossby wave dynamics, and eyewall process) and external environmental conditions (e.g., uniform environmental flow, vertical shear in the environmental wind, moisture distribution, and land surface process) (Wang et al., 1998; Wang and Wu, 2004). The SST magnitude and horizontal gradient of SST affect both internal and external dynamics on TC motion. For example, the SST-induced change in vertical wind shear is related to both the vertically titled internal structure and external environmental flow effects. These SST effects may include the interaction between internal and external dynamics. Wang and Wu (2004) have shown that the external environmental flow affects the TC structure change through the inner core processes. To separate the internal dynamics from external dynamics, model simulation should be performed in the absence of large-scale environmental factors and surface fluxes. The detailed dynamics on relative contribution between internal and external dynamics and their interaction process are out of our scope, which will be investigated in the future study.

The SST magnitude significantly strengthens the TC intensity through the enhanced thermodynamic energy supply. While the response is almost monotonic, there is a slight change in the intensity below an SST of ~300 K. The SST

value may be related to the SST threshold for TC formation and development suggested in Wendland (1977). In relation to the change in the TC track, a warmer SST induces a greater eastward drift in the TC motion. The asymmetry in the PVT, which has the maximum to the northeast and the minimum to the southwest, suggests that the TC tends to move toward the northeast. A warmer SST leads a larger eastward deflection of the maximum PVT. The change in the PVT is primarily contributed by the HA term of the PV. The DH term makes a weak contribution to the TC motion, which is likely to be in part due to a dominant cyclonic rotation in the rainfall. The southwesterly flow, which is enhanced relative to the SST magnitude, could advect the cyclonic vortex northeastward more effectively.

On the other hand, the zonally increased SST in the translating direction generates a larger eastward deflection of the TC motion than the meridional SST gradient and the SST magnitude. The increased SSTs in the moving direction provide a more favorable condition for the southwestward tilt of the vortex axis and the resultant vertical easterly/southerly wind shear. Consequently, the greater eastward drift in the TC motion is related to the development of the asymmetric vortex and flow, caused by the vertical tilt of the vortex axis. Although the insignificant impact of the meridionally increased SST is not yet explained, it may be related to the asymmetries in the air–sea energy exchanges shown in Chang and Madala (1980). Indeed, the effect of the vertical wind shear on the TC track has not been firmly demonstrated yet (e.g., Jones, 1995; Zheng et al., 2007). This is an indicator that both the vertical wind shear and vertical structure of the TC play an important role in determining the TC tracks. In this study, the asymmetric structure of TC in relation to the vertical wind shear modulates the northeastward movement of TCs. Further investigation in this regard must be carried out in future studies.

The conclusions in this paper are not valid for overall typhoons in the East Asia. Since the experiments are done in the environmental condition for a real TC case, the SST effect on TC track may be in part influenced by the complex environmental interaction such as the mid-latitude trough interaction. To confirm the SST impact isolated from the environmental interaction, the effects of SST should be examined in more real TC cases, and this remains a topic for further study. Despite the interaction process, the results in the present study are reasonably consistent with those in simple idealized experiments on SST impact (Chang and Madala, 1980). In the northeastward-moving TCs around East Asia, the mean flow surrounding the TC center appears to play a more important role in determining the TC motion than does the beta effect. The relative contribution of the mean flow and the beta effect will be examined in a future study. In addition, the TC motion is affected by many other factors such as the basic environmental flow and the air–sea interaction. For example, how sensitive the SST impact on TC track to changing environmental flow should be addressed. The effects of such factors should be investigated in more detail in a future study. This study could provide a better understanding of the dynamical mechanisms responsible for the TC track in real environmental factors around East Asia. Understanding the dynamical process of TC track under different SST distributions may contribute to accurate prediction of TC motion around East Asia.

Acknowledgments

This research was supported by a grant from "Construction of Ocean Research Stations and their Application Studies" funded by the Ministry of Land, Transport and Maritime Affairs of Korean government. Work of JCLC was funded by the Research Grants Council of the Hong Kong Special Administrative Region of China Grant CityU 100210.

References

Adem, J., 1956. A series solution for the barotropic vorticity equation and its application in the study of atmospheric vortices. Tellus 8, 64–372.
Au-Yeung, A.Y.M., Chan, J.C.L., 2010. The effect of a river delta and coastal roughness variation on a landfalling tropical cyclone. J. Geophys. Res. 115, D19121. doi:10.1029/2009JD013631.
Bender, M.A., 1997. The effect of relative flow on the asymmetric structure in the interior of hurricanes. J. Atmos. Sci. 54, 703–724.
Black, M.L., Gamache, J.F., Marks Jr., F.D., Samsury, C.E., Willoughby, H.E., 2002. Eastern Pacific Hurricanes Jimena of 1991 and Olivia of 1994: the effect of vertical shear on structure and intensity. Mon. Weather Rev. 130, 2291–2312.
Chan, J.C.L., Williams, R.T., 1987. Analytical and numerical studies of the beta-effect in tropical cyclone motion, part I: zero mean flow. J. Atmos. Sci. 44, 1257–1265.
Chan, J.C.L., Duan, L.Y., Shay, L.K., 2001. Tropical cyclone intensity change from a simple ocean–atmosphere coupled model. J. Atmos. Sci. 58, 154–172.
Chan, J.C.L., Ko, F.M.F., Lei, Y.M., 2002. Relationship between potential vorticity tendency and tropical cyclone motion. J. Atmos. Sci. 59, 1317–1336.
Chang, S.W., Madala, R.V., 1980. Numerical simulation of the influence of sea surface temperature on translating tropical cyclones. J. Atmos. Sci. 37, 2617–2630.
Emanuel, K.A., 1986. An air–sea interaction theory for tropical cyclones. Part I: steady-state maintenance. J. Atmos. Sci. 43, 585–604.
Fiorino, M.J., Elsberry, R.L., 1989. Some aspects of vortex structure related to tropical cyclone motion. J. Atmos. Sci. 46, 975–990.
Flatau, M., Schubert, W.H., Stevens, D.E., 1994. The role of baroclinic processes in tropical cyclone motion: The influence of vertical tilt. J. Atmos. Sci. 51, 2589–2601.
Frank, W.M., Ritchie, E.A., 2001. Effects of vertical wind shear on the intensity and structure of numerically simulated hurricanes. Mon. Weather Rev. 129, 2249–2269.
Holland, G.J., 1997. The maximum potential intensity of tropical cyclones. J. Atmos. Sci. 54, 2519–2541.
Hong, S.-Y., Noh, Y., Dudhia, J., 2006. A new vertical diffusion package with an explicit treatment of the entrainment processes. Mon. Weather Rev. 124, 2318–2341.
Jones, S.C., 1995. The evolution of vortices in vertical shear. I: Initially barotropic vortices. Q. J. R. Meteorol. Soc. 121, 821–851.
Kain, J.S., Fritsch, J.M., 1990. A one-dimensional entraining/detraining plume model and its application in convective parameterization. J. Atmos. Sci. 47, 2784–2802.
Kuo, H.C., Williams, R.T., Chen, J.H., Chen, Y.L., 2001. Topographic effects on barotropic vortex motion: no mean flow. J. Atmos. Sci. 58, 1310–1327.
Marks, F.D., Shay, L.K., 1998. Landfalling tropical cyclones: forecasting problems and associated research opportunities. Bull. Am. Meteorol. Soc. 79, 305–323.
Pereira Filho, A.J., Pezza, A.B., Simmonds, I., Lima, R.S., Vianna, M., 2010. New perspectives on the synoptic and mesoscale structure of Hurricane Catarina. Atmos. Res. 95, 157–171.
Ritchie, E.A., Frank, W.M., 2007. Interactions between simulated tropical cyclones and an environment with a variable coriolis parameter. Mon. Weather Rev. 135, 1889–1905.
Tuleya, R.E., Kurihara, Y., 1982. A note on the sea surface temperature sensitivity of a numerical model of tropical storm genesis. Mon. Weather Rev. 110, 2063–2069.
Wang, Y., Holland, G.J., 1996. Tropical cyclone motion and evolution in vertical shear. J. Atmos. Sci. 53, 3313–3332.

Wang, Y., Wu, C.-C., 2004. Current understanding of tropical cyclone structure and intensity changes—a review. Meteorol. Atmos. Phys. 87, 257–278.
Wang, B., Russell, L.E., Wang, Y., Wu, L., 1998. Dynamics in tropical cyclone motion: a review. Chin. J. Atmos. Sci. 22, 416–434.
Wendland, W.M., 1977. Tropical storm frequencies related to sea surface temperatures. J. Appl. Meteorol. 16, 477–481.
Willoughby, H.E., 1990. Linear normal modes of a moving, shallow-water barotropic vortex. J. Atmos. Sci. 47, 2141–2148.
Wong, M.L.M., Chan, J.C.L., 2004. Tropical cyclone intensity in vertical wind shear. J. Atmos. Sci. 61, 1859–1876.
Wong, M.L.M., Chan, J.C.L., 2006. Tropical cyclone motion in response to land surface friction. J. Atmos. Sci. 63, 1324–1337.
Wu, L., Wang, B., 2000. A potential vorticity tendency diagnostic approach for tropical cyclone motion. Mon. Weather Rev. 128, 1899–1911.
Wu, L., Wang, B., Braun, S.A., 2005. Impacts of air–sea interaction on tropical cyclone track and intensity. Mon. Weather Rev. 133, 3299–3314.
Zheng, X., Duan, Y.H., Yu, H., 2007. Dynamical effects of environmental vertical wind shear on tropical cyclone motion, structure, and intensity. Meteorol. Atmos. Phys. 97, 207–220.